

OPTIMAL CONTROL OF A FLEXIBLE ROBOT ARM

JAMES D. LEE and BEN-LI WANG

Robot Systems Division, National Bureau of Standards, Gaithersburg, MD 20899, U.S.A.

(Received 6 August 1987)

Abstract—This work is a computer simulation of the control of a flexible robot arm. The dynamic equations for a single-link flexible robot arm have been derived rigorously. This arm has two degrees of freedom in rotation and one in translation so that the workspace is three-dimensional. The payload is simulated by attaching additional mass to the arm at a specified location. The governing equations of the plant and the measurements are nonlinear. The process of control is divided into two stages: coarse control and fine control. Based on the optimal control theory, a linear observer is constructed for fine control. The numerical results are presented here.

INTRODUCTION

Most of today's industrial robots can lift only about one-twentieth of their own weight. Compare that to the human arm which can lift about ten times its own weight. The top slew velocity of a robot arm is typically around 40 inches per second while the top slew velocity that can be achieved by the human arm during a task such as throwing a baseball is around 1500 inches per second. Although these comparisons may not be fair, the point stands that there is vast room for improvement in the performance of robotic manipulators. One of the most elementary problems in robotics is that of accuracy. The repeatability of most of today's robots is of the order of 1 mm over the working space, the accuracy of absolute positioning (for the end effector to reach the commanded point) may be off as much as 1 cm. The present solution to the problem of accuracy is to make robot structures very stiff and rigid. Another problem in robotics is control. Nowadays, in order to position the end effector to the commanded location the angles that each of the robot's joints must assume are computed and then the joints are driven simultaneously to said angles. After the joint angles assume those computed values, the robot is presumed stiff enough so that the end effector will thus (by dead reckoning) be in the intended location. Therefore, not only are the robots built to be massive and unwieldy, the analysis and the controls in robotics are based on the assumption that the robot arm is just a collection of rigid bodies.

It is desirable to build a lightweight robot arm which has a long reach and the capability to carry a heavy payload and to move rapidly. In order to meet these requirements, the robot arm has to be flexible. In other words, even the static deflection of the robot arm has to be taken into account for positioning accuracy; more importantly, the high moving speed of the arm implies the inertia forces acting on the arm are very large and the stability of the robot arm becomes a critical problem which requires the engineers to design a more sophisticated control

system. In the area of control of flexible robot arms, Cannon and Schmitz [1] published the pioneer work in 1984. In that work the mathematical modeling and the initial experiments have been carried out to address the control of a flexible member (one link of a robot system) where the position of the end effector (tip) is controlled by measuring that position and using the measurement as a basis for applying control torque to the other end of the flexible member (joint). Also, it is worthwhile mentioning the works of Harashima and Ueshiba [2], Wang and Vidyasagar [3, 4], Sangveraphunsiri [5] and Book *et al.* [6]. In all the above-mentioned works, two things are common: the one-link robot arm, with its hub rotating about the z -axis, sweeps the horizontal x - y plane; the flexible arm is modeled as a beam whose deflection is represented by a series in terms of eigenfunctions (normal modes).

In this work, the computer simulation of the control of a single-link flexible robot arm is presented. The hub of the arm can rotate about the z -axis, specified by the joint angle $\theta(t)$, and the y' -axis, specified by the joint angle $\phi(t)$. Also, the arm can slide along its own longitudinal axis, so that the working region of the end effector is a three-dimensional space instead of a circle on the horizontal plane. The flexible arm is divided into a number of beam elements and then treated by finite element method to obtain the governing equations for the mechanical system. By doing so, it is more flexible and natural to incorporate payloads into the system. Moreover, it will be seen later that the system (plant), including the measurement of the tip position, is nonlinear and there is no attempt being made to linearize that.

PROBLEM DESCRIPTION

The single-link robot arm being considered in this work is shown in Fig. 1. The arm consists of two parts: the hub, which is modeled as a rigid body, and the flexible beam, which is further divided into n

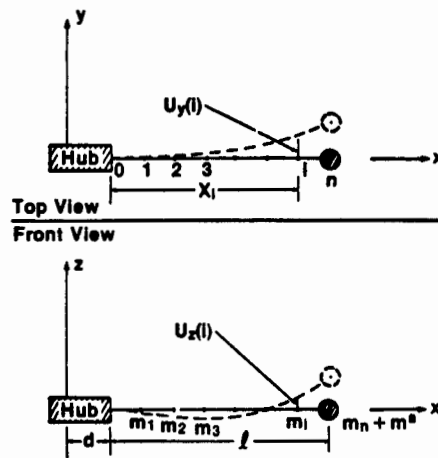


Fig. 1. Single-link robot arm in its home configuration.

beam elements. The flexible beam is in the shape of a slim hollow cylinder with length l , outer radius r_o and inner radius r_i . A rectangular coordinate system (x, y, z) , in which the z -axis is opposite to the direction of gravity, is employed in this work. The configuration, in which the axis of the hub as well as the axis of the beam in its undeformed state is parallel to the x -axis, is named the home configuration. The differences in position between the deformed state and the undeformed state of the beam in the home configuration are the displacements (U_y, U_z) referring to the home configuration as indicated in the figure. Not only can the flexible beam deform, the hub can rotate about the z -axis and the y' -axis, which is perpendicular to the axis of the hub and the z -axis, and can also slide along its own axis. The rotations of the arm about the z -axis and the y' -axis are specified by two time-dependent variables, $\theta(t)$ and $\phi(t)$, respectively. However, in this work, the sliding of the arm is specified by a constant parameter, d , which is determined by the given target position, as being discussed later. Since the flexible beam is modeled as n beam elements, it has $n + 1$ nodal points. The generic i th nodal point ($i = 0, 1, 2, \dots, n$) is associated with the lumped mass, m_i , and referring to the home configuration, the coordinates $[X_i + d, U_y(i), U_z(i)]$. The payload is simulated by the mass attached to the end point (the n th nodal point), m^a , as indicated in the figure. The computer software developed at NBS allows the payload to be carried at all nodal points, hence, from now on unless otherwise stated, the lumped mass, m_i , stands for the sum of the payload carried at the i th nodal point and the mass of the beam distributed to that nodal point.

TRANSFORMATIONS

The position vector of any point on the beam, when it is in the home configuration, can be expressed

as

$$\mathbf{x} \equiv \begin{bmatrix} X + d \\ U_y \\ U_z \end{bmatrix} \quad (1)$$

The rotation of the hub about the z -axis and the y' -axis transforms the arm from its home configuration to its actual configuration, as shown in Fig. 2. The transformation may be expressed by the following equation

$$\begin{aligned} \mathbf{x}^* &\equiv \begin{bmatrix} x^* \\ y^* \\ z^* \end{bmatrix} \\ &= \begin{bmatrix} \sin \phi \cos \theta & -\sin \theta & -\cos \phi \cos \theta \\ \sin \phi \sin \theta & \cos \theta & -\cos \phi \sin \theta \\ \cos \phi & 0 & \sin \phi \end{bmatrix} \\ &\quad \times \begin{bmatrix} X + d \\ U_y \\ U_z \end{bmatrix} \\ &\equiv \mathbf{Q}\mathbf{x}. \end{aligned} \quad (2)$$

It is noticed that \mathbf{Q} is an orthogonal transformation matrix which has the following properties

$$\begin{aligned} \mathbf{Q}^{-1} &= \mathbf{Q}^T, \\ \det(\mathbf{Q}) &= 1. \end{aligned} \quad (3)$$

In other words, any vector \mathbf{V}^* , in the actual configuration, can be transformed into \mathbf{V} , the corresponding vector in the home configuration, through $\mathbf{V} = \mathbf{Q}^T \mathbf{V}^*$.

Now the velocity and the acceleration, \mathbf{v}^* and \mathbf{a}^* , can be obtained as

$$\mathbf{v}^* \equiv \frac{d\mathbf{x}^*}{dt} = \dot{\mathbf{Q}}\mathbf{x} + \mathbf{Q}\mathbf{v}, \quad (4)$$

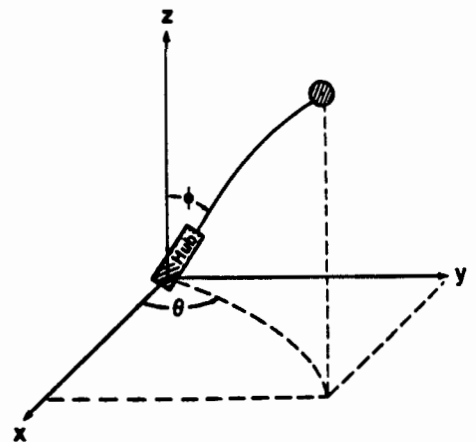


Fig. 2. Single-link robot arm in its actual configuration.

$$\begin{aligned} \mathbf{a}^* &\equiv \begin{bmatrix} a_x^* \\ a_y^* \\ a_z^* \end{bmatrix} \equiv \frac{d\mathbf{v}^*}{dt} \\ &= \ddot{\mathbf{Q}}\mathbf{x} + 2\dot{\mathbf{Q}}\mathbf{v} + \mathbf{Q}\mathbf{a}, \end{aligned} \quad (5)$$

where

$$\mathbf{v} \equiv \frac{d\mathbf{x}}{dt} = \begin{bmatrix} 0 \\ \dot{U}_y \\ \dot{U}_z \end{bmatrix}, \quad (6)$$

$$\mathbf{a} \equiv \frac{d\mathbf{v}}{dt} = \begin{bmatrix} 0 \\ \ddot{U}_y \\ \ddot{U}_z \end{bmatrix}. \quad (7)$$

INERTIA FORCE AND GRAVITY

The total force acting on a generic nodal point, \mathbf{f}^* , is equal to the sum of the inertia force and the gravitational force acting on that point, i.e.,

$$\mathbf{f}^* = \begin{bmatrix} f_x^* \\ f_y^* \\ f_z^* \end{bmatrix} = -m \begin{bmatrix} a_x^* \\ a_y^* \\ a_z^* \end{bmatrix} + mg \begin{bmatrix} 0 \\ 0 \\ -1 \end{bmatrix}, \quad (8)$$

where m is the effective mass lumped at that nodal point; and g , the constant of gravity, is equal to 32.2 ft/sec². The corresponding force in the home configuration, \mathbf{f} , can be obtained as

$$\begin{aligned} \mathbf{f} &= \begin{bmatrix} f_x \\ f_y \\ f_z \end{bmatrix} = \mathbf{Q}^T \mathbf{f}^* \\ &= -m \left\{ \mathbf{P}\mathbf{x} + \mathbf{R}\mathbf{v} + \mathbf{a} + g \begin{bmatrix} \cos \phi \\ 0 \\ \sin \phi \end{bmatrix} \right\}, \end{aligned} \quad (9)$$

where

$$\begin{aligned} \mathbf{P} &\equiv \mathbf{Q}^T \ddot{\mathbf{Q}} \\ &= \begin{bmatrix} -\sin^2 \phi \theta^2 - \dot{\phi}^2 & -\sin \phi \ddot{\theta} \\ \sin \phi \ddot{\theta} + 2 \cos \phi \dot{\phi} \dot{\theta} & -\theta^2 \\ -\dot{\phi} + \sin \phi \cos \phi \theta^2 & \cos \phi \ddot{\theta} \\ \dot{\phi} + \sin \phi \cos \phi \theta^2 & \\ -\cos \phi \ddot{\theta} + 2 \sin \phi \dot{\phi} \dot{\theta} & \\ -\cos^2 \phi \theta^2 - \dot{\phi}^2 & \end{bmatrix}, \end{aligned} \quad (10)$$

$$\begin{aligned} \mathbf{R} &\equiv 2\mathbf{Q}^T \dot{\mathbf{Q}} \\ &= \begin{bmatrix} 0 & -2 \sin \phi \dot{\theta} & 2 \dot{\phi} \\ 2 \sin \phi \dot{\theta} & 0 & -2 \cos \phi \dot{\theta} \\ -2 \dot{\phi} & 2 \cos \phi \dot{\theta} & 0 \end{bmatrix}. \end{aligned} \quad (11)$$

For example, when $\phi = \pi/2$ and $\dot{\phi} = \ddot{\phi} = 0$, the following is obtained

$$f_y = -m \{ \ddot{U}_y + \ddot{\theta}(X+d) - \theta^2 U_y \}. \quad (12a)$$

However, correspondingly, the inertia force obtained by Cannon and Schmitz [1], Harashima and Ueshiba [2] and Wang and Vidyasagar [3, 4] may be written as

$$f_y = -m \{ \ddot{U}_y + \ddot{\theta}(X+d) \}; \quad (12b)$$

in other words, the nonlinear term $m\theta^2 U_y$ has been omitted. This example indicates that the expressions of the inertia force and gravity obtained in this work contain no approximation and are more general than those obtained in [1-4].

FINITE ELEMENT ANALYSIS

The generic i th beam element connects the $(i-1)$ th nodal point and the i th nodal point, as shown in Fig. 3. Based on elementary beam theory, the governing equation of this element may be written as [7-9]:

$$\mathbf{K}^i \begin{bmatrix} U_{i-1} \\ U_i \\ S_{i-1} \\ S_i \end{bmatrix} = \begin{bmatrix} f_{i-1} \\ f_i \\ M_{i-1} \\ M_i \end{bmatrix}, \quad (13)$$

where the local stiffness matrix of the i th element is expressed as

$$\mathbf{K}^i = \frac{EI}{l_i^3} \begin{bmatrix} 12 & -12 & 6l_i & 6l_i \\ -12 & 12 & -6l_i & -6l_i \\ 6l_i & -6l_i & 4l_i^2 & 2l_i^2 \\ 6l_i & -6l_i & 2l_i^2 & 4l_i^2 \end{bmatrix}; \quad (14)$$

E is the Young's modulus; $l_i \equiv X_i - X_{i-1}$; I is the moment of inertia; for the i th nodal point, U_i is the displacement $U_y(U_z)$, $S_i = dU_i/dX$ is the slope, f_i is the acting force $f_y(f_z)$, M_i is the moment about the z - (y -) axis.

The global stiffness matrix of the beam is the assembly of all the local stiffness matrices. The boundary condition of a cantilever beam is that the displacement and the slope are zero at the fixed end. After this boundary condition is imposed, the governing equations for the beam may be expressed

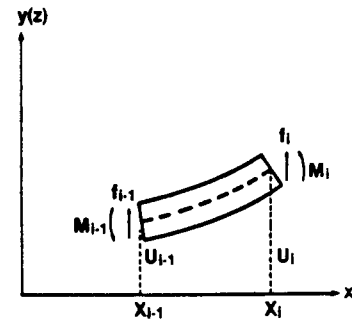


Fig. 3. The generic i th beam element.

as

$$\mathbf{K}_a \mathbf{U} + \mathbf{K}_b \mathbf{S} = \mathbf{f}, \quad (15)$$

$$\mathbf{K}_c \mathbf{U} + \mathbf{K}_d \mathbf{S} = \mathbf{M}, \quad (16)$$

where

$$\mathbf{U} \equiv (U_1, U_2, \dots, U_n)^T,$$

$$\mathbf{S} \equiv (S_1, S_2, \dots, S_n)^T,$$

$$\mathbf{f} \equiv (f_1, f_2, \dots, f_n)^T,$$

$$\mathbf{M} \equiv (M_1, M_2, \dots, M_n)^T.$$

Since there is no moment acting on the beam, i.e. $\mathbf{M} = 0$, eqn (16) implies that

$$\mathbf{S} = -\mathbf{K}_d^{-1} \mathbf{K}_c \mathbf{U}. \quad (17)$$

Substituting eqn (17) into eqn (15), the following is obtained

$$\mathbf{K} \mathbf{U} = \mathbf{f}, \quad (18)$$

where the stiffness matrix, \mathbf{K} , can be calculated as

$$\mathbf{K} = \mathbf{K}_a - \mathbf{K}_b \mathbf{K}_d^{-1} \mathbf{K}_c. \quad (19)$$

In view of eqn (9), eqn (18) can be rewritten as

$$\dot{\mathbf{U}} + \mathbf{m}^{-1} \mathbf{K} \mathbf{U} = \mathbf{F}, \quad (20)$$

where \mathbf{m} is the mass matrix, i.e. $\mathbf{m} = \text{diag.}(m_1, m_2, \dots, m_n)$; \mathbf{F} is the vector of forcing terms. If U_i stands for the displacement $U_y(U_x)$ at the i th nodal point, then F_i stands for the forcing term $F_y(F_x)$ and

$$\begin{aligned} F_y(i) = & -(\sin \phi \ddot{\theta} + 2 \cos \phi \dot{\phi} \dot{\theta}) (X_i + d) \\ & + \theta^2 U_y(i) - (-\cos \phi \ddot{\theta} + 2 \sin \phi \dot{\phi} \dot{\theta}) \\ & \times U_x(i) + 2 \cos \phi \theta \dot{U}_x(i), \end{aligned} \quad (21)$$

$$\begin{aligned} F_x(i) = & -(-\ddot{\phi} + \sin \phi \cos \phi \dot{\theta}^2) (X_i + d) \\ & - \cos \phi \ddot{\theta} U_y(i) + (\cos^2 \phi \dot{\theta}^2 + \dot{\phi}^2) \\ & \times U_x(i) - 2 \cos \phi \theta \dot{U}_y(i) - g \sin \phi. \end{aligned} \quad (22)$$

It is noticed that, if θ and ϕ are given as functions of time, eqn (20) can be readily solved by invoking the Runge-Kutta method or other appropriate numerical methods. However, as it will be seen later, θ , $\dot{\theta}$, ϕ , and $\dot{\phi}$ are regarded as state variables and the governing equations for the flexible robot arm as a control problem will be formulated in the next sections.

TARGET

Consider the displacements, $U_y(i)$ and $U_x(i)$, the velocities, $\dot{U}_y(i)$ and $\dot{U}_x(i)$, the joint angles, θ and ϕ ,

the angular velocities, $\dot{\theta}$ and $\dot{\phi}$, as the state variables of the system. Consider the angular accelerations, $\ddot{\theta}$ and $\ddot{\phi}$, or the torques, T_θ and T_ϕ , as control variables of the system. The purpose of the control is to find the control laws that make the system converge to a steady state which meets certain prescribed requirements. If the solutions are converging, then, as time approaches infinity, the time derivatives of all the variables approach zero, and

$$\lim_{t \rightarrow \infty} [U_y(t), U_x(t), \theta(t), \phi(t)] = [U_y^f, U_x^f, \theta^f, \phi^f]. \quad (23)$$

According to eqn (20), it is seen that

$$\dot{U}_i^f = 0, \quad (24)$$

$$\mathbf{m}^{-1} \mathbf{K} \mathbf{U}_i^f = -g \sin \phi^f. \quad (25)$$

In order for the end effector to reach the given target position (x^f, y^f, z^f) , eqn (2) becomes

$$\begin{bmatrix} x^f \\ y^f \\ z^f \end{bmatrix} = \begin{bmatrix} \sin \phi^f \cos \theta^f & -\sin \theta^f & -\cos \phi^f \cos \theta^f \\ \sin \phi^f \sin \theta^f & \cos \theta^f & -\cos \phi^f \sin \theta^f \\ \cos \phi^f & 0 & \sin \phi^f \end{bmatrix} \times \begin{bmatrix} l + d \\ 0 \\ \Delta \end{bmatrix}, \quad (26)$$

which can be rewritten as

$$\theta^f = \theta^f = \tan^{-1}(y^f/x^f), \quad (27)$$

$$(l + d)^2 + \Delta^2 = (x^f)^2 + (y^f)^2 + (z^f)^2 = (r^f)^2, \quad (28)$$

$$\cos \phi^f (l + d) + \sin \phi^f \Delta = z^f, \quad (29)$$

where l is the length of the flexible beam, $\Delta \equiv U_x^f(n)$ is the displacement of the end effector. From eqns (25, 28, 29), U_x^f , ϕ^f , and d can be determined.

TORQUES

The torque about the z -axis, T_θ , and the torque about the y' -axis, T_ϕ , can be evaluated as

$$\begin{aligned} T_\theta = & \sum_{i=0}^n [f_x^* y^* - f_y^* x^*]_i + [I_h + m_h (L_h/2 - d)^2] \\ & \times (\sin^2 \phi \ddot{\theta} + 2 \sin \phi \cos \phi \dot{\phi} \dot{\theta}), \end{aligned} \quad (30)$$

$$\begin{aligned} T_\phi = & \sum_{i=0}^n [f_z^* (x^* \cos \theta + y^* \sin \theta) \\ & - z^* (f_x^* \cos \theta + f_y^* \sin \theta)]_i \\ & + [I_h + m_h (L_h/2 - d)^2] (\ddot{\phi} - \sin \phi \cos \phi \dot{\theta}^2) \\ & + m_h g (L_h/2 - d) \sin \phi, \end{aligned} \quad (31)$$

where I_h , m_h and L_h , are the moment of inertia, the mass, and the length of the hub, respectively; (x^*, y^*, z^*) are the coordinates of the nodal point, which can be calculated by eqn (2); (f_x^*, f_y^*, f_z^*) are the forces acting on that nodal point, which can be calculated by eqn (8).

It is noticed that eqns (30) and (31) are very complicated since the effect of deformation on the torque is incorporated in the formulation. If the effect of deformation on the torques is neglected, then T_θ and T_ϕ are reduced to

$$T_\theta \approx T'_\theta = (\sin^2 \phi \ddot{\theta} + 2 \sin \phi \cos \phi \dot{\phi} \dot{\theta}) \times \left\{ \sum_{i=0}^n m_i (X_i + d)^2 + [I_h + m_h (L_h/2 - d)^2] \right\}, \quad (32)$$

$$T_\phi \approx T'_\phi = (\ddot{\phi} - \sin \phi \cos \phi \dot{\theta}^2) \left\{ \sum_{i=0}^n m_i (X_i + d)^2 + [I_h + m_h (L_h/2 - d)^2] \right\} + g \sin \phi \left\{ m_h (L_h/2 - d) - \sum_{i=0}^n m_i (X_i + d) \right\}. \quad (33)$$

For converging solutions, it is seen that, as time approaches infinity, T_θ and T'_θ approach zero, and

$$\Delta T_\phi \equiv \lim_{t \rightarrow \infty} (T_\phi - T'_\phi) = \left[\sum_{i=0}^n m_i U_i'(i) \right] g \cos \phi', \quad (34)$$

which is a measure of the effect of deformation on the torque in the static case.

If it is feasible to consider $\ddot{\theta}$ and $\ddot{\phi}$ as control variables, then it is straightforward, as it will be seen later, to formulate the control laws; moreover, the torques, T_θ and T_ϕ , can be calculated according to eqns (30) and (31), taking the effect of deformation into consideration. On the other hand, if torques are taken as the control variables and one is willing to make an approximation, i.e. to neglect the effect of deformation on the torques, then eqns (32) and (33) can be expressed as

$$\ddot{\theta} = g_1(\alpha) T'_\theta + g_2(\alpha), \quad (35)$$

$$\ddot{\phi} = h_1 T'_\phi + h_2(\alpha), \quad (36)$$

where α stands for all the state variables. Now, eqns (35) and (36) and eqn (20) form a complete set of governing equations for the control system. However, it is felt that the effect of deformation on the torques should be considered in the treatment for the sake of consistency. In this work, the angular accelerations are taken as the control variables and in the forth-

coming paper, the torques, which include the effect of deformation, will be taken as the control variables.

EQUATIONS OF THE SYSTEM

Define two vectors of state variables as follows

$$\alpha_1 \equiv [U_y(1), U_y(2), \dots, U_y(n), \theta', \dot{U}_y(1), \dot{U}_y(2), \dots, \dot{U}_y(n), \theta], \quad (37)$$

$$\alpha_2 \equiv [U'_z(1), U'_z(2), \dots, U'_z(n), \phi', \dot{U}'_z(1), \dot{U}'_z(2), \dots, \dot{U}'_z(n), \phi], \quad (38)$$

where

$$\theta' \equiv \theta - \theta'$$

$$\phi' \equiv \phi - \phi'$$

$$U'_z(i) \equiv U_z(i) - U'_z(i), \quad i = 1, 2, \dots, n. \quad (39)$$

Then the governing equations of the system can be written as

$$\dot{\alpha}_1 = \mathbf{A}_1 \alpha_1 + \mathbf{B}_1 u_1 + \mathbf{N}_1(\alpha_1, \alpha_2, u_1, u_2), \quad (40)$$

$$\dot{\alpha}_2 = \mathbf{A}_2 \alpha_2 + \mathbf{B}_2 u_2 + \mathbf{N}_2(\alpha_1, \alpha_2, u_1, u_2), \quad (41)$$

where

$$\mathbf{B}_1 = [0, 0, \dots, 0, b_1(1), b_1(2), \dots, b_1(n), 1]^T, \quad (42)$$

$$b_1(i) = -\sin \phi'(X_i + d) + \cos \phi' U'_z(i), \quad (43)$$

$$\mathbf{B}_2 = [0, 0, \dots, 0, b_2(1), b_2(2), \dots, b_2(n), 1]^T, \quad (44)$$

$$b_2(i) = X_i + d, \quad (45)$$

$$\mathbf{N}_1 = [0, 0, \dots, 0, N_1(1), N_1(2), \dots, N_1(n), 0]^T, \quad (46)$$

$$N_1(i) = [(\sin \phi' - \sin \phi)(X_i + d) + \cos \phi U_z(i) - \cos \phi' U'_z(i)] \ddot{\theta} + \theta^2 U_y(i) + 2 \cos \phi \theta \dot{U}_y(i) - 2[\cos \phi(X_i + d) + \sin \phi U_z(i)] \phi \dot{\theta}, \quad (47)$$

$$\mathbf{N}_2 = [0, 0, \dots, 0, N_2(1), N_2(2), \dots, N_2(n), 0]^T, \quad (48)$$

$$N_2(i) = -\cos \phi U_y(i) \ddot{\theta} + [\cos^2 \phi U_z(i) - \sin \phi \cos \phi(X_i + d)] \dot{\theta}^2 + U_z(i) \phi^2 - 2 \cos \phi \theta \dot{U}_y(i) - g[\sin \phi - \sin \phi' - \cos \phi'(\phi - \phi')], \quad (49)$$

$$u_1 = \theta', \quad (50)$$

$$u_2 = \phi', \quad (51)$$

and the nonvanishing components of the two $(2n+2) \times (2n+2)$ matrices, A_1 and A_2 , are

$$\begin{aligned} (A_1)_{ij} &= (A_2)_{ij} = 1, \\ 1 \leq i \leq n+1, \quad j &= i+n+1 \\ (A_1)_{ij} &= (A_2)_{ij} = (-m^{-1}K)_{ij}, \\ 1 \leq j \leq n, \quad n+2 \leq i \leq 2n+1 \\ (A_2)_{ij} &= -g \cos \phi', \quad j = n+1, \\ n+2 \leq i \leq 2n+1. \end{aligned} \quad (52)$$

From eqns (40) and (41) it is seen that the angular accelerations, θ' and ϕ' , are taken as the control variables; also, all the nonlinear terms are contained in the functions N_1 and N_2 which have the following property

$$\begin{bmatrix} N_1 \\ N_2 \end{bmatrix} \rightarrow 0 \quad \text{as} \quad \begin{bmatrix} \theta(t) \\ \phi(t) \\ U_y(t) \\ U_z(t) \end{bmatrix} \rightarrow \begin{bmatrix} \theta' \\ \phi' \\ 0 \\ U'_z \end{bmatrix}. \quad (53)$$

From now on, the governing equations of the system, eqns (40) and (41), may be written symbolically as

$$\dot{\alpha} = A\alpha + Bu + N(\alpha_1, \alpha_2, u_1, u_2). \quad (54)$$

THE MEASUREMENTS

It is assumed that the position and the velocity of the end effector, (x_n^*, y_n^*, z_n^*) and (v_x^*, v_y^*, v_z^*) , can be measured. Recall eqns (2, 4) and eqn (26) as follows:

$$\begin{aligned} \begin{bmatrix} x_n^* \\ y_n^* \\ z_n^* \end{bmatrix} &= Q \begin{bmatrix} l+d \\ U_y(n) \\ U_z(n) \end{bmatrix}, \\ \begin{bmatrix} v_x^* \\ v_y^* \\ v_z^* \end{bmatrix} &= \dot{Q} \begin{bmatrix} l+d \\ U_y(n) \\ U_z(n) \end{bmatrix} + Q \begin{bmatrix} 0 \\ \dot{U}_y(n) \\ \dot{U}_z(n) \end{bmatrix}, \quad (55) \\ \begin{bmatrix} x' \\ y' \\ z' \end{bmatrix} &= Q' \begin{bmatrix} l+d \\ 0 \\ U'_z(n) \end{bmatrix}. \quad (56) \end{aligned}$$

Then the difference between the position of the end effector and the target position can be obtained as

$$\begin{bmatrix} \Delta x^* \\ \Delta y^* \\ \Delta z^* \end{bmatrix} = \begin{bmatrix} x_n^* - x' \\ y_n^* - y' \\ z_n^* - z' \end{bmatrix}. \quad (57)$$

Define a vector, δ , as follows:

$$\delta = (\delta_1, \delta_2, \delta_3, \delta_4, \delta_5, \delta_6)^T, \quad (58)$$

$$\begin{bmatrix} \delta_1 \\ \delta_2 \\ \delta_3 \end{bmatrix} = (Q')^T \begin{bmatrix} \Delta x^* \\ \Delta y^* \\ \Delta z^* \end{bmatrix}$$

$$= (Q')^T Q \begin{bmatrix} l+d \\ U_y(n) \\ U_z(n) \end{bmatrix} - \begin{bmatrix} l+d \\ 0 \\ U'_z(n) \end{bmatrix}. \quad (59)$$

$$\begin{bmatrix} \delta_4 \\ \delta_5 \\ \delta_6 \end{bmatrix} = (Q')^T \begin{bmatrix} v_x^* \\ v_y^* \\ v_z^* \end{bmatrix}$$

$$= (Q')^T \dot{Q} \begin{bmatrix} l+d \\ U_y(n) \\ U_z(n) \end{bmatrix} + (Q')^T Q \begin{bmatrix} 0 \\ \dot{U}_y(n) \\ \dot{U}_z(n) \end{bmatrix}. \quad (60)$$

It is seen that δ is a nonlinear function of the state variables. If a Taylor series expansion of δ is performed about the final position, $(\theta = \theta', \phi = \phi', U_y = 0, U_z = U'_z)$ the linear expressions of δ is obtained as

$$\delta_1 \approx U'_z \phi' \quad (61)$$

$$\delta_2 \approx U_y(n) + [\sin \phi'(l+d) - \cos \phi' U'_z(n)] \theta', \quad (62)$$

$$\delta_3 \approx U'_z(n) - (l+d) \phi', \quad (63)$$

$$\delta_4 \approx U'_z \phi', \quad (64)$$

$$\delta_5 \approx \dot{U}_y(n) + [\sin \phi'(l+d) - \cos \phi' U'_z(n)] \dot{\theta}', \quad (65)$$

$$\delta_6 \approx \dot{U}_z(n) - (l+d) \dot{\phi}'. \quad (66)$$

Now the governing equations and the measurements of the system in linear form can be symbolically written as

$$\dot{\alpha} = A\alpha + Bu, \quad (67)$$

$$\delta = H\alpha, \quad (68)$$

where A, B, H are constant matrices, based on which the estimator will be constructed.

THE CONTROL

In order to construct a controller and an observer based on the optimal control theory, first, let the equations of the system (plant) and the measurements be written as

$$\dot{\alpha} = A\alpha + Bu + N + v, \quad (69)$$

$$y = \delta(\alpha) + w \approx H\alpha + w, \quad (70)$$

where v is the state excitation (white) noise vector; w is the measurement (white) noise vector. Also, let the

performance criterion be expressed as

$$I = \int_0^{\infty} [\alpha^T(\tau)R_1\alpha(\tau) + u^T(\tau)R_2u(\tau)] d\tau, \quad (71)$$

where R_1 and R_2 are called the state weighting matrix and control weighting matrix, respectively.

It is assumed that all the noises considered in this work are uncorrelated and the variance matrices defined as

$$V \equiv E\{v(t)v^T(t)\}, \quad (72)$$

$$W \equiv E\{w(t)w^T(t)\}, \quad (73)$$

are constants in time.

Now, let the observer and the control law be represented by

$$\dot{\hat{\alpha}} = \hat{A}\hat{\alpha} + \hat{B}u + L(\gamma - \hat{H}\hat{\alpha}), \quad (74)$$

$$u = -C\hat{\alpha}, \quad (75)$$

where C and L are called the control gain matrix and estimate gain matrix, respectively; $\hat{\alpha}$, the estimates of α , are the state variables of the estimator (observer); and, with the symbol “ $\hat{}$ ” on top of A , B and H , it is emphasized that the number of beam elements, \hat{n} , for constructing the estimator may be different from (far less than) that for simulating the system.

Following the derivations by Kwakernaak and Sivan [10], or by Friedland [11], the control gain and the estimate gain can be computed as follows. First, define matrices Y and Z as

$$Y \equiv \begin{bmatrix} \hat{A} & -\hat{B}R_2^{-1}\hat{B}^T \\ -R_1 & -\hat{A}^T \end{bmatrix}, \quad (76)$$

$$Z \equiv \begin{bmatrix} \hat{A}^T & -\hat{H}^T W^{-1} \hat{H} \\ -V & -\hat{A} \end{bmatrix}. \quad (77)$$

Let the matrix p and the matrix q be composed of the eigenvectors of Y and Z , respectively, i.e. the i th column vector of $p(q)$ is the eigenvector of $Y(Z)$ corresponding to the i th eigenvalue of $Y(Z)$. Let p and q be partitioned as

$$p = \begin{bmatrix} p_1^+ & p_1^- \\ p_2^+ & p_2^- \end{bmatrix}, \quad (78)$$

$$q = \begin{bmatrix} q_1^+ & q_1^- \\ q_2^+ & q_2^- \end{bmatrix}, \quad (79)$$

where $p^+(q^+)$ and $p^-(p^-)$ are eigenvectors corresponding to eigenvalues with positive real part and negative real part, respectively. Now, the control gain matrix and the estimate gain matrix can be written as

$$C = R_2^{-1}\hat{B}^T\lambda, \quad (80)$$

$$L = \beta\hat{H}^T W^{-1}, \quad (81)$$

where

$$\lambda = p_2^-(p_1^-)^{-1}, \quad (82)$$

$$\beta = q_2^-(q_1^-)^{-1}. \quad (83)$$

If there had been no nonlinear function, N , in eqn (69) and no difference between $\delta(\alpha)$ and $H\alpha$ in eqn (70), then the properly obtained gain matrices, C and L , would have guaranteed the convergency and the stability of the solutions; in other words, the end effector eventually would have reached the target position asymptotically. Now, on the contrary, it is noticed that N approaches zero and δ approaches $H\alpha$ only if (θ, ϕ, U_y, U_z) approach $(\theta^f, \phi^f, 0, U_z^f)$. Therefore, eqns (74) and (75) may be referred as *fine control*; eqn (75) is then named the fine control law. As *coarse control* is concerned, which is the first-stage control, eqns (74) and (75) are replaced by

$$\dot{\hat{\alpha}} = \hat{A}\hat{\alpha} + \hat{B}u + \hat{N}(\hat{\alpha}_1, \hat{\alpha}_2, u_1, u_2), \quad (84)$$

$$\dot{\theta} = c_1(\theta^f - \theta) - d_1\dot{\theta}, \quad (85)$$

$$\dot{\phi} = c_2(\phi^f - \phi) - d_2\dot{\phi}, \quad (86)$$

where the last two equations may be named the coarse control laws; c_1, c_2, d_1 and d_2 are positive constants; the nonlinear function \hat{N} in eqn (84) may be omitted. One shifts from coarse control to fine control at time t_1 as soon as the following condition is met

$$|\hat{\theta}(t_1) - \theta^f| \leq \theta^e, \quad |\hat{\phi}(t_1) - \phi^f| \leq \phi^e, \quad (87)$$

where θ^e and ϕ^e are input parameters set by the designer of the control system. In this work, $\theta^e = \phi^e = 5^\circ$. $c_1 = c_2 = 0.5/\text{sec}^2$, $d_1 = d_2 = 0.2/\text{sec}$. The block diagrams of the system and the estimator for coarse control and fine control are shown in Figs 4 and 5, respectively.

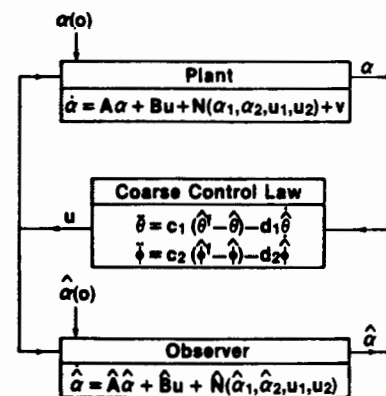


Fig. 4. The block diagram of coarse control.

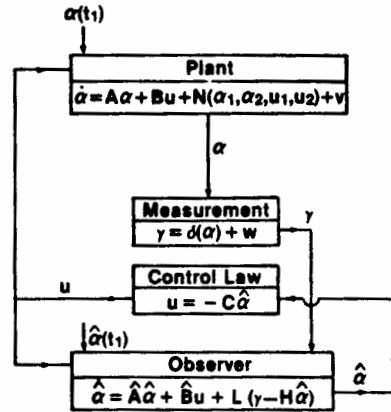


Fig. 5. The block diagram of fine control.

NUMERICAL RESULTS

In this section, for illustrative purposes, the numerical results of two cases are presented. In the following, the input parameters are set to be

- (a) material: aluminum

$$E = 10^7 \text{ psi}, \quad \rho = 0.2536 \times 10^{-3} \text{ lb/in.}^3,$$

- (b) geometry of the flexible arm

$$r_0 = 2 \text{ in.}, \quad r_i = 1.9 \text{ in.},$$

- (c) payload

$$m^a = 40 \text{ lbf},$$

- (d) target position

$$\theta' = \phi' = 45^\circ,$$

- (e) initial joint angles

$$\theta(0) = 0^\circ, \quad \phi(0) = 90^\circ,$$

- (f) number of beam elements

$$n = 8 \text{ (plant)}$$

$$\hat{n} = 4 \text{ (observer),}$$

- (g) controller/observer

$$W = \text{diag. } [0.01, 0.01, 0.01, 0.1, 0.1, 0.1]$$

- (1) for $\alpha = \alpha_1$, [eqn (37)]

$$R_1 = \text{diag. } [1100, 4400, 9900,$$

$$17600, 22 \times 10^6, 1.1, 4.4, 9.9, 17.6, 1100]$$

$$R_2 = 400$$

$$V = \text{diag. } [0.005, 0.01, 0.015, 0.02, \\ 0.0005, 0.5, 1.0, 1.5, 2.0, 0.0005]$$

- (2) for $\alpha = \alpha_2$, [eqn (38)]

$$R_1 = \text{diag. } [500, 1000, 1500, 2000, \\ 4000, 1, 2, 3, 4, 4000]$$

$$R_2 = 400$$

$$V = \text{diag. } [0.0025, 0.005, 0.0075, 0.01, \\ 0.00025, 0.25, 0.5, 0.75, 1.0, 0.00025].$$

In Figs 6–7, the joint angles $\theta(\phi)$ (solid lines) and the tip angles $\theta_{\text{tip}}(\phi_{\text{tip}})$ (solid lines with marks) are shown as functions of time. The tip angles are defined as

$$\theta_{\text{tip}} = \tan^{-1}(y_n^*/x_n^*), \quad (88)$$

$$\phi_{\text{tip}} = \cos^{-1}(z_n^*/\sqrt{(x_n^*)^2 + (y_n^*)^2 + (z_n^*)^2}). \quad (89)$$

In Fig. 6 it is noticed that the settling time, t_s , is about 6 sec; the shift from coarse control to fine control occurs at $t_1 = 2.36$ sec; $\phi' = 41.15^\circ$; the ratio of payload with respect to the weight of the flexible arm is equal to 0.925. It is well known that if the magnitudes of V and W are increased or decreased by multiplying a factor, R , the poles of $\hat{A} - L\hat{H}$ do not change their locations; in other words, the estimate gain does not change. However, the levels of white

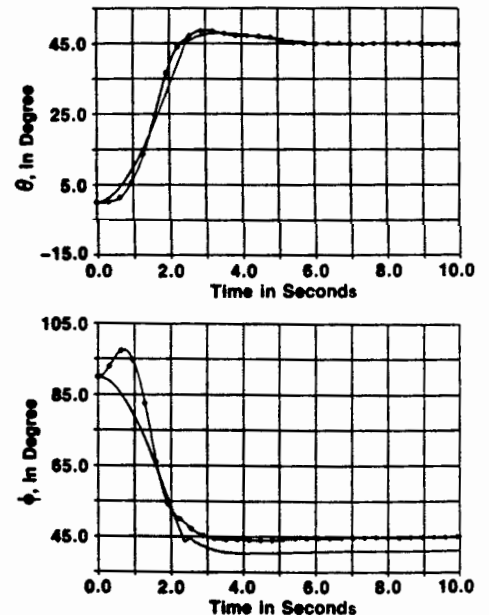


Fig. 6. Responses of joint angles and tip angles. $l = 360$ inches, $r_0 = 2$ inches, $r_i = 1.9$ inches, $r' = 370$ inches, $c_1 = c_2 = 0.5/\text{sec}^2$, $d_1 = d_2 = 0.2/\text{sec}$.

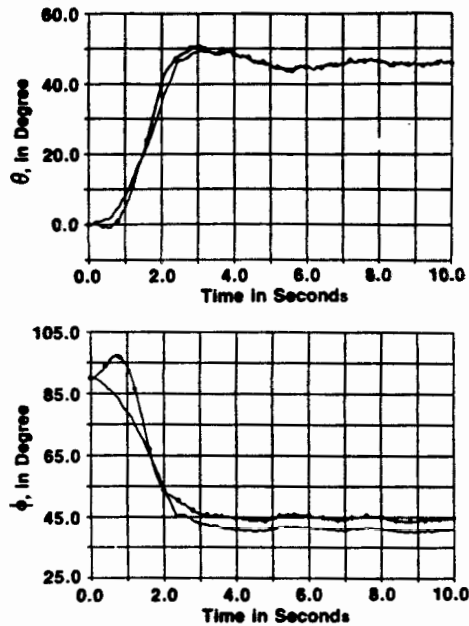


Fig. 7. Responses of joint angles and tip angles. $l = 360$ inches, $r_o = 2$ inches, $r_f = 1.9$ inches, $r' = 370$ inches, $c_1 = c_2 = 0.5/\text{sec}^2$, $d_1 = d_2 = 0.2/\text{sec}$. $R = 100.0$.

noises, v and w , are changed and hence the response of the system, plotted in Fig. 7, is changed. In Fig. 7 it is seen that the controller works but, because of the existence of a large amount of white noise, the tip of the flexible arm oscillates restlessly about the target position.

DISCUSSION

In this work the single-link flexible robot arm has two degrees of freedom for rotations (θ and ϕ) and one degree of freedom for sliding (d) so that the space, which can be reached by the end effector, is three-dimensional. In the analysis, θ and ϕ are treated as variables, but the sliding, d , is treated as a parameter, i.e. a constant determined by the given target position.

The time-dependent white noises, $v(t)$ and $w(t)$, which appear in eqns (69) and (70), are generated by invoking a random number generator with the variance matrices V and W specified by the designer of the control system.

The governing equations of the system (plant) and the equations representing the measurements, which have been derived rigorously, are nonlinear. No attempt whatsoever has been made to linearize those

equations. However, the estimator (observer) was constructed based on the linear version of the system. Also, it is noticed that the number of beam elements used to model the plant, n , and the observer, \hat{n} , may be different; for example, for the cases reported in this work, $n = 8$ and $\hat{n} = 4$. This means the observer is linear and involves very few variables. For practical purposes, it implies that real-time control of flexible robot arm is feasible.

If damping is included in the system, one may prove that even a very simple coarse control law serves the purpose to control the flexible robot arm by setting the joint angles at precalculated values and letting nature (in this case, damping) take its course. However, the settling time is too long to be practical. On the other hand, as it becomes clear in this study, the combination of the coarse control and the fine control works even if the system has no damping at all. Generally speaking, as has been pointed out by Book *et al.* [6], damping in the robot arm made of most practical materials is influential on higher modes, but not on the dominant mode of the arm. It is suggested that engineers do not count on damping for the purpose of controlling the flexible robot arm.

REFERENCES

1. R. H. Cannon, Jr and E. Schmitz, Initial experiments on the end-point control of a flexible one-link robot. *Int. J. Robotics Res.* 3, 62-75 (1984).
2. F. Harashima and T. Ueshiba, Adaptive control of flexible arm using the end-point sensing. Proceedings, Japan-U.S.A. Symposium on Flexible Automation, Osaka, Japan, July 1986, pp. 225-229.
3. D. Wang and M. Vidyasagar, Modelling and control of a flexible beam using the stable factorization approach (private communication).
4. D. Wang and M. Vidyasagar, Control of a flexible beam for optimum step response (private communication).
5. V. Sangveraphunsiri, The optimal control and design of a flexible manipulator arm. Thesis, School of Mechanical Engineering, Georgia Institute of Technology, Atlanta, GA (1984).
6. W. J. Book, T. E. Alberts and G. G. Hastings, Design strategies for high-speed lightweight robot. *Comput. Mech. Engng* 26-33 (1986).
7. J. S. Przemieniecki, *Theory of Matrix Structural Analysis*. McGraw-Hill, New York (1968).
8. P. Tong and J. N. Rossettos, *Finite-Element Method Basic Technique and Implementation*. MIT Press, Cambridge, MA (1977).
9. F. L. Stansa, *Applied Finite Element Analysis for Engineers*. Holt, Reinhart & Winston, New York (1985).
10. H. Kwakernaak and R. Sivan, *Linear Optimal Control Systems*. John Wiley, New York (1972).
11. B. Friedland, *Control System Design An Introduction to State-Space Methods*. McGraw-Hill, New York (1986).